Environmental Effects on Anion Polarizability: Variation with Lattice Parameter and Coordination Number

Patrick Jemmer and Patrick W. Fowler*

Department of Chemistry, University of Exeter, Stocker Road, Exeter EX4 4QD, U.K.

Mark Wilson and Paul A. Madden

Physical and Theoretical Chemistry Laboratory, Oxford University, South Parks Road, Oxford OX1 3QZ, U.K.

Received: April 28, 1998

The results of ab initio calculations of in-crystal ionic polarizabilities, α, over a wide range of lattice parameters, *R*, are presented for LiF, NaF, KF, LiCl, NaCl, KCl, LiBr, NaBr, KCl, and MgO. The derivatives of the mean polarizability with respect to lattice parameters are compared with experimental values obtained from the variation of the refractive index with pressure. The environmental effects on the polarizability of an anion may be viewed as the consequence of imposition of a confining potential on its electron density whose origin includes Coulombic interactions and the exclusion of these electrons from the region occupied by the electron density of the first-neighbor shell of cations. This model suggests scaling relationships, between values of $\alpha(R)$ obtained at different levels of calculation and for a given anion with different cations, which are shown to be semiquantitative. These findings lead to the proposal of a universal representation of the polarizability of a given anion, which predicts the dependence on lattice parameter and crystal form and transfers from one substance to another.

1. Introduction

Anions in crystals are known from calculation and experiment to be different from their free counterparts: they are smaller, less polarizable, and more strongly bound. The physical picture underlying this effect is one in which the polarizability of a compressible, negative ion is affected by the number and distribution of its neighbors. The pseudopotential arising from the neighbors constitutes a "box" confining the anionic electron density, as discussed in detail in refs 1−3. In-crystal anionic polarizabilities are thus not constant but are, rather, functions of the environment. It is possible to obtain calculated results for ionic polarizabilities that are in excellent agreement with experiment by taking a free ion and embedding it in a simulation of the crystalline environment (with "real" nearest neighbors and point charges for more distant ions).[4] Such simulations can be used to explain the variation in properties between free, surface, and in-crystal ions and between ions in different crystals.[5−8] Models incorporating these insights can be used to derive consistent empirical ionic polarizabilities and dispersion coefficients for predicting crystal refractive indexes and energies.[9]

The purpose of the present investigation is to explore the behavior of the mean polarizability α for a series of anions and cations over a wide range of lattice separations, *R*. Specifically, we investigate the functional dependence on the crystalline environment of the properties of the halide ion, X^-, in MX (M = Li, Na, and K; X = F, Cl, and Br) and of the O^{2-} ion in MgO. We have previously treated the polarizabilities of these anions at the equilibrium crystal geometries and considered their variation with geometric distortion in several cases.[3−6] Calculations with varying lattice parameters have been carried out around the equilibrium geometries of several polymorphs by Pyper and Popelier for α (O^{2-} in MgO).[8] In the present calculations, we shall simulate the effect of a continuous isotropic expansion of the crystalline lattice. For *R* in the vicinity of the equilibrium lattice spacing, $\alpha(R)$ may be compared with experimental data from the pressure dependence of the refractive index. The broader objective of the work is to establish the validity of the confining potential model illustrated in Figure 1. This model makes specific predictions about the form of the *R*-dependence of the anion polarizability. The simplest, one-electron model calculations[10,11] suggest simple universal forms for this polarizability function, with sigmoid or monotonically rising functions for systems that would be respectively bound or unbound in free space. The model further indicates how the polarizabilities of a given anion in different

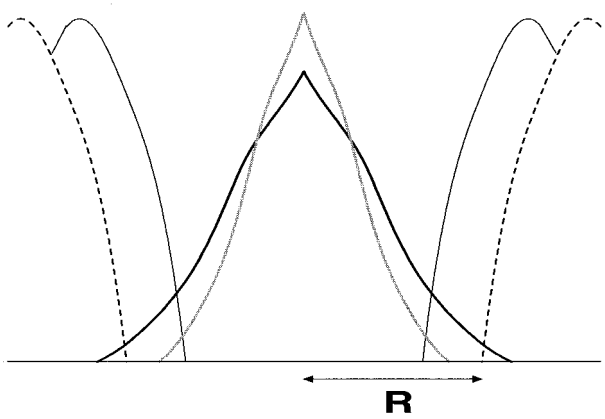

Figure 1. Origin of the spherical confining potential which acts on the electrons around an anion in a cubic crystal. A cross section through the spherical potential, V_0, is shown: the dashed line shows the Coulombic (Madelung) contribution, associated with the point ionic charges. This is enhanced by the exclusion from the region occupied by the electron density of the other ions. V_0 compresses the free anion charge density (heavy line) to the in-crystal charge density (light line).

10.1021/jp982029j CCC: $15.00
Published on Web 10/06/1998

materials should be related, since the size of the confining box should depend only on the lattice parameter and the radius of the cation electron density. Such predictions may be examined with the calculated data.

The model is suggestive of universal forms to represent the dependence of the polarizability of an anion on interatomic separations. These provide a means of calculating the polarizability in an arbitrary coordination environment and enable the parametrization of interionic potential energy functions,[12,13] predicting light-scattering spectra[14] inter alia. We will propose such functions in the present work and compare the predictions with measured and calculated anion polarizabilities in different crystalline environments.

The paper is divided into three main sections. First, the calculations are described. Second, the calculated quantities will be compared directly with experiment. The third section considers the construction of an appropriate model for $\alpha(R)$ and its extension to include coordination number dependence.

In addition to studying the dependence of the dipolar polarizability on R, we will also present a more limited study of the dependence of the quadrupole polarizability, C, on lattice parameters. Recent molecular dynamics studies have highlighted a potentially significant role for the induced quadrupoles in determining both static crystalline[15,16] and dynamic properties.[17,18] These studies have been impeded by the relative scarcity of literature data for C. An understanding of $C(R)$ would be a first step in rectifying these omissions.

2. Ab Initio Calculations

Ab initio calculations were performed using the Cambridge Analytic Derivatives Package, CADPAC,[19] and the Exeter version of the SYSMO package[20] on ion clusters embedded in point charge lattice fragments for the systems listed earlier. These follow closely our previous methodology, established in equilibrium and distortion studies of LiF and other alkali halides. Calculations were performed where possible at both the self-consistent-field (SCF)[19,20] and the second-order correlated Møller−Plessett (MP2) level.[19]

The techniques used to perform the analysis described above and to extract the required geometric derivatives are extensions of our earlier work[3,4,6] on the in-crystal properties of the F^- ion in distorted and undistorted LiF lattices. It was found there that a useful way of extracting information on the environmental effects on the central F^- anion in LiF, for example, is to consider a rocksalt (B1) $[(F^-)(Li^+)_6]^{5+}$ cluster embedded in a $5 \times 5 \times 5$ cube of point charges, with scaled charges on the outer faces chosen to ensure charge neutrality and to approximate the correct Madelung potential[21] at the central anion site. These calculations are of the type called CLUS in previous work and model both short- and long-range environmental effects. To distinguish between pure electrostatic and overlap effects, subsidiary calculations are performed on the simpler so-called CRYS systems, where the anion is embedded in the bare point charge lattice and so has no extended charge clouds on its cationic neighbors.

To provide a good description of the ionic species in the crystalline environment, some attention must be paid to the choice of basis set. For the anions, the sets used are as follows: O^{2-} (14s9p5d3f),[22] F^- (15s10p5d3f)/[12s8p5d3f],[5] Cl^- (16s13p6d3f)/[13s11p5d3f],[5] and Br^- (16s12p6d2f)/[11s10p5d2f].[7] For the cations: Mg^{2+} (10s8p)/[2s1p],[22] Li^+ (10s5p)/[1s1p],[4] Na^+ (10s8p)/[2s1p],[5] and K^+ (14s9p2d)/[3s2p1d].[5] The anion basis sets are flexible and represent the electron distribution, its response to the crystal and to external fields, and the variation of that response in the crystal. The cation basis sets are intended to represent the electron distribution of the "hard" cation and (by incorporating contractions of p-functions in the case of Li^+ and contractions of d-functions in the case of K^+) its polarizability, both of which are insensitive to the crystalline environment.

Ab initio calculations of this kind produce dipole polarizabilities, α^{CLUS}, that are properties of the ion clusters as a whole. This overall polarizability can be apportioned to the constituent ions by a method described previously.[3,4,6] The polarizability may be calculated for the empty cation "cage" alone, giving α^{CAGE}, which may itself be subject to basis set superposition error (BSSE), for which correction procedures are available.[23] The contribution of the central anion, α, may then be calculated by subtraction as

$$\alpha = \alpha^{CLUS} - \alpha^{CAGE} - \alpha^{DID} \tag{2.1}$$

A first-order dipole−induced dipole correction for the rocksalt structure,[4] α^{DID},

$$\alpha^{DID} = 12\alpha_+\alpha_-{}^2 R^{-6} \tag{2.2}$$

was made to the dipole polarizability, to allow for the mutual enhancement of polarizability that would exist even for point ions in proximity. The raw polarizabilities α_+ and α_- used in this correction are calculated either for an ion in a point charge lattice or by an iterative procedure based on the overall CLUS value.

In the case of the Li^+, K^+, and Mg^{2+} systems, the BSSE contribution to the total CAGE quantities was estimated to be small, due to low either intrinsic cation polarizability (for Li^+ and Mg^{2+}) or the nature of the cation basis set (in the case of K^+), and was not explicitly considered. However, in the case of NaX systems, BSSE is potentially more important, as the cation basis contains no polarization functions, and, where possible, an estimate was obtained by performing a counterpoise correction using either the full set of X^- orbitals (which produces an upper bound) or the X^- df-orbital sets (which produces an approximate lower bound).

A similar process was carried out to obtain the anion quadrupole polarizabilities, $\mathbf{C}$:

$$\mathbf{C} = \mathbf{C}^{CLUS} - \mathbf{C}^{CAGE} \tag{2.3}$$

In these cases, no dipole−induced dipole corrections were required since, in the basis sets used, the intrinsic quadrupole polarizabilities of the cations are vanishingly small. In octahedral symmetry, the $\mathbf{C}$ tensor for the central anion has two independent components:[24] the trace

$$C = \frac{1}{5}C_{\alpha\beta,\alpha\beta} = \frac{3}{5}(C_{zz,zz} + 2C_{xy,xy}) \tag{2.4}$$

and the aniostropy,

$$\Delta C = \frac{3}{2}C_{zz,zz} - 2C_{xy,xy} \tag{2.5}$$

The interpretation of the ab initio polarizability calculations rests on certain key assumptions. It is first assumed that the cations are "frozen"; that is, they undergo no relaxation as the lattice expands.[3−6] This invariance is guaranteed in our calculations by the choice of highly contracted cation basis sets. All the space generated between cations by the expansion of the lattice is, therefore, assumed to be available for expansion

TABLE 1: Free Ion (α_∞) and Equilibrium Lattice Parameter Dipole Polarizabilties (α_e) Calculated at SCF and MP2 Levels in Both the CLUS and CRYS Environments[a]

		α_e (a_0^3)				α_∞ (a_0^3)	
		SCF		MP2			
system	R (a_0)	CRYS	CLUS	CRYS	CLUS	SCF	MP2
LiF	3.7965	7.5715	5.4139	9.7012	6.3486	10.6548	16.8384
NaF	4.3785	8.6020	5.9702−6.0682	11.6594	7.2076−7.3113		
KF	5.0512	9.5687	6.7045	13.7672			
LiCl	4.8566	24.9554	18.8784	27.5173	19.9838	31.4474	37.4183
NaCl	5.3290	26.9690	19.9126	30.2535	21.1580		
KCl	5.9451	28.7588		32.8663			
LiBr	5.1968	32.2016	26.4565	33.8170	27.3572	38.2862	41.7209
NaBr	5.6427	33.8369	27.8033−27.6068	35.7823	28.6233−28.8256		
KBr	6.2361	35.3265		37.6449			
MgO	3.9760	24.5440	11.1776	32.1198			

[a] All values are quoted in a_0^3. The CLUS(MP2) calculations on NaX systems indicate the spread obtainable by using different estimates of BSSE where possible (see text).

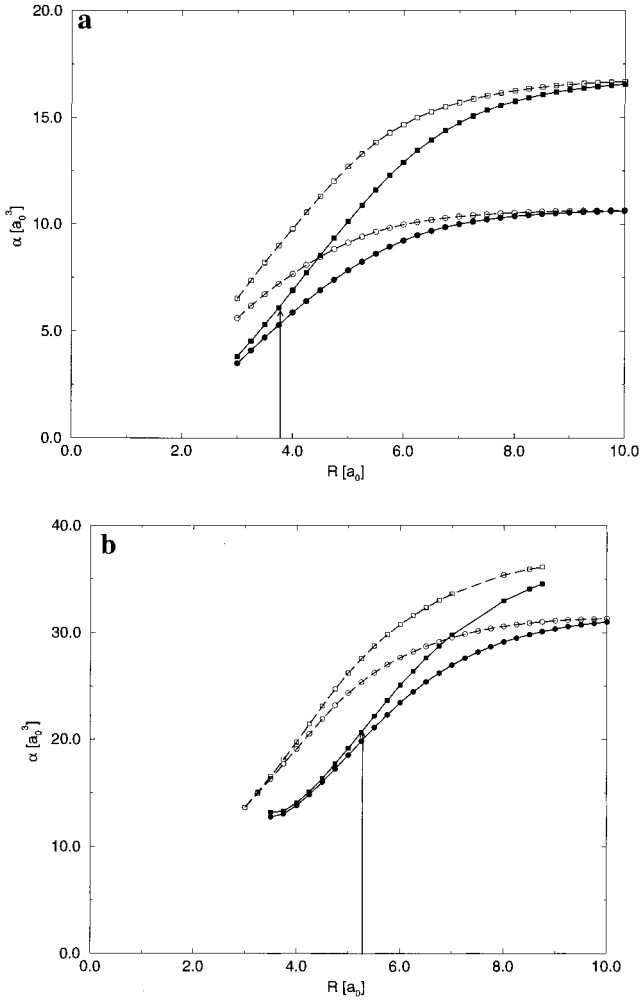

Figure 2. Representative ab initio SCF/MP2 dipole polarizabilities as a function of R calculated in both the CRYS and CLUS environments for (a) F^- in LiF and (b) Cl^- in NaCl. Key: ○, CRYS(SCF); ●, CLUS-(SCF); □, CRYS(MP2); ■, CLUS(MP2). The arrows indicate the location of the equilibrium lattice parameter and experimental anion polarizability.

of the anion, and all the variation in the total polarizability is attributable to anion polarizability functions, $\alpha_-(R)$. This is enforced by the decomposition recipe outlined above. The validation of such a procedure arises from comparing CLUS and CRYS calculations. The relationship between these calculations should, and does, give an indication of cation size.

TABLE 2: Experimental Polarizability Derivatives and Refractive Indexes[a]

system	n	$\rho(dn/d\rho)$	Λ_0	$-V_m(d\epsilon/dV_m)$	$(d\alpha/dR)$ (a_0^2)	ref
LiF	1.389	0.124−0.130			3.423−3.490	25
			0.65−0.715		3.21−3.53	34
				0.366	3.374	27
				0.40	3.28	30
LiCl	1.670			0.573	9.852	28
LiBr	1.794			0.653	13.305	28
LiI	1.972			0.828	18.667	28
NaF	1.323	0.124			3.59	26
				0.488	2.584	27
				0.33	3.492	30
NaCl	1.533	0.255−0.280			6.73−7.21	25
				0.74	7.617	31
				0.85	6.986	30
				0.846	7.011	27
NaBr	1.625			0.99	9.619	30
				0.986	9.644	27
NaI	1.755			1.28	13.602	28
KF	1.364			0.509	4.315	28
KCl	1.483			0.68	8.447	31
				0.84	7.095	30
				0.93	6.335	27
KBr	1.546			1.08	8.083	31
				1.01	8.676	30
				1.098	7.931	27
KI	1.637			1.40	10.412	31
				1.28	11.436	30
				1.443	10.045	27
RbF	1.393			0.565	5.148	28
RbCl	1.483			1.031	5.996	27
				1.01	6.190	31
				1.05	5.821	30
RbBr	1.536			1.215	7.148	27
				1.24	6.914	30
RbI	1.616			1.432	9.904	27
				1.31	10.113	30
MgO	1.367		1.23−1.28		11.435−11.900	35

[a] The numbers are quoted in the dimensionless form used in the particular experimental report, and then converted in column 6 to an equivalent derivative $d\alpha/dR$ using lattice parameters as quoted in Table 1.

3. Ab Initio Results

Halides. The results in the form of the polarizability of the ion at the equilibrium lattice parameter (α_e) and as a free ion are given in Table 1. The values of $d\alpha/dR$, calculated by a five-point central difference formula with step size $0.005a_0$, will be given later in Table 3.

Two representative sets of curves $\alpha(R)$ for the halides LiF and NaCl are shown in Figure 2. They illustrate the general

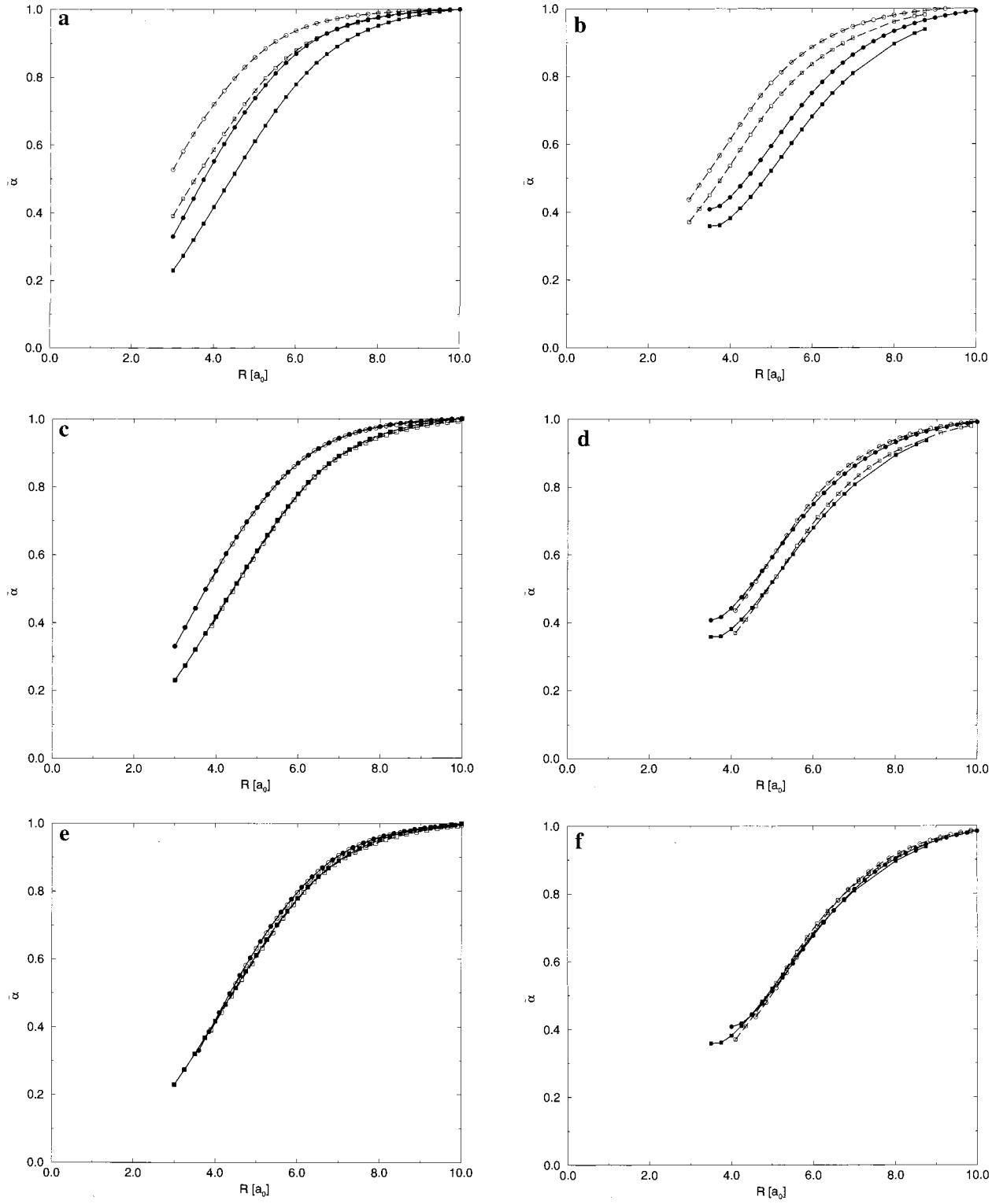

Figure 3. Three scaling procedures required to produce the "universal" $\tilde{\alpha}(R)$ curve. In panels a and b, the ab initio data from Figure 2 are divided by the free ion polarizability (Table 1). In panels c and d, the CRYS curves are shifted along R by δ_{M^+} ($0.9a_0$ and $1.2a_0$ for Li^+ and Na^+, respectively). In panels e and f, the scaling procedure is finalized by shifting the SCF curves along R by $0.5a_0$ and $0.6a_0$, respectively. The symbols used are as in Figure 2, and the ordinate, $\tilde{\alpha}$, is the scaled polarizability as discussed in the text (section 3, Halides).

trends found for all the halide calculations. In all cases, the polarizability increases with interionic separation and is greater in the point charge CRYS simulation than in the full CLUS calculation. This reflects the two-fold (electrostatic plus overlap) source of compression for the anion illustrated in Figure 1.

For technical reasons (poor convergence of couterpoise corrections), the CLUS (MP2) polarizability curve (Figure 2) and derivatives (Tables 1 and 2) presented for NaCl refer to a smaller basis, in which all *f*-functions on Cl^- had been removed. Numerical experiments with Cl^- in LiCl show that the *f*-functions affect the scaled polarizability derivatives by, at most, 2%, and so the values quoted for NaCl should be close approximations to the full basis result.

Polarizability values from the correlated MP2 calculations are larger than the corresponding SCF values. The enhancement $\alpha(\text{MP2}) - \alpha(\text{SCF})$ increases with R, an indication of the large

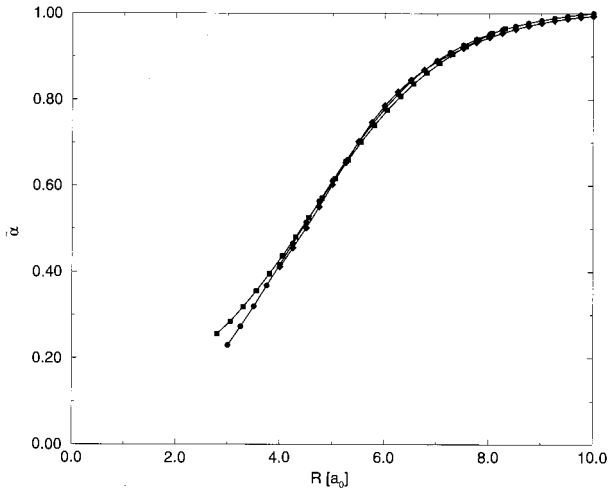

Figure 4. Three "universal" $\tilde{\alpha}(R)$ curves for F^-, Cl^-, and Br^-. Key: ●, F^-; ■, Cl^-; ◆, Br^-.

contribution of radial correlation to the polarizability of the free ion which is quenched as the separation is reduced.[4]

The halide anions at all levels of calculation show a generally sigmoid polarizability curve, as expected for bound systems: at small distance, the compressive effect of the crystalline "box" masks the detail of the particular intraionic potential; at intermediate distances, there is a smooth, roughly linear increase in polarizability; and at sufficiently large distance, the polarizability reaches the limiting value for the free system.[10,11] The generic nature of this behavior is illustrated by the fact that the curves for all the halide ions at each level of approximation can be reduced to a "universal" form by first scaling with respect to the free ion polarizability and then translating along the separation axis.

The stages in this process are illustrated in Figure 3 for F^- in LiF. Division by the respective values of the free ion polarizability (Table 1) gives a set of four resolved curves converging to the same limit (Figure 3) and with an ordering of the scaled polarizabilities, $\tilde{\alpha} \equiv \alpha/\alpha_\infty$, where α_∞ is the polarizability of the free anion calculated at the appropriate level of theory and of simulation of the environment: $\tilde{\alpha}_{SCF}^{CRYS} > \tilde{\alpha}_{MP2}^{CRYS} > \tilde{\alpha}_{SCF}^{CLUS} > \tilde{\alpha}_{MP2}^{CLUS}$.

The observations that $\tilde{\alpha}_{SCF}^{CRYS} > \tilde{\alpha}_{SCF}^{CLUS}$ and $\tilde{\alpha}_{MP2}^{CRYS} > \tilde{\alpha}_{MP2}^{CLUS}$ for a given cation are consistent with the model of the environmental effects illustrated in Figure 1. For a given interionic separation R, the width of the "box" available for the electrons of the anion is smaller for the CLUS calculation than for the CRYS, because in the former the anion's electrons are excluded from the region of space occupied by the electrons of the first coordination shell of cations. This model is suggestive of further scaling of the polarizability data, since $\tilde{\alpha}_{SCF}^{CLUS}$ calculated at R should be similar to $\tilde{\alpha}_{SCF}^{CRYS}$ at a separation smaller than R by δ_{M^+}, where δ_{M^+} is a characteristic radius of the cationic charge density. The same should be true of the relationship between $\tilde{\alpha}_{MP2}^{CRYS}$ and $\tilde{\alpha}_{MP2}^{CLUS}$.

Application of a positive translation $R \rightarrow R + \delta_{M^+}$ to the two CRYS curves results in a pair of near-coincident curves, one for the SCF and one for the MP2 levels of calculation (Figure 3b). δ_{M^+} is chosen to bring the CRYS and CLUS curves into exact coincidence at the equilibrium lattice parameter. From the discussion above, it would be anticipated that the same shift would be required to bring the SCF and MP2 curves into coincidence, and this is found to be the case. Furthermore, the values of the shifts δ_{M^+} are expected to reflect the cation radii.

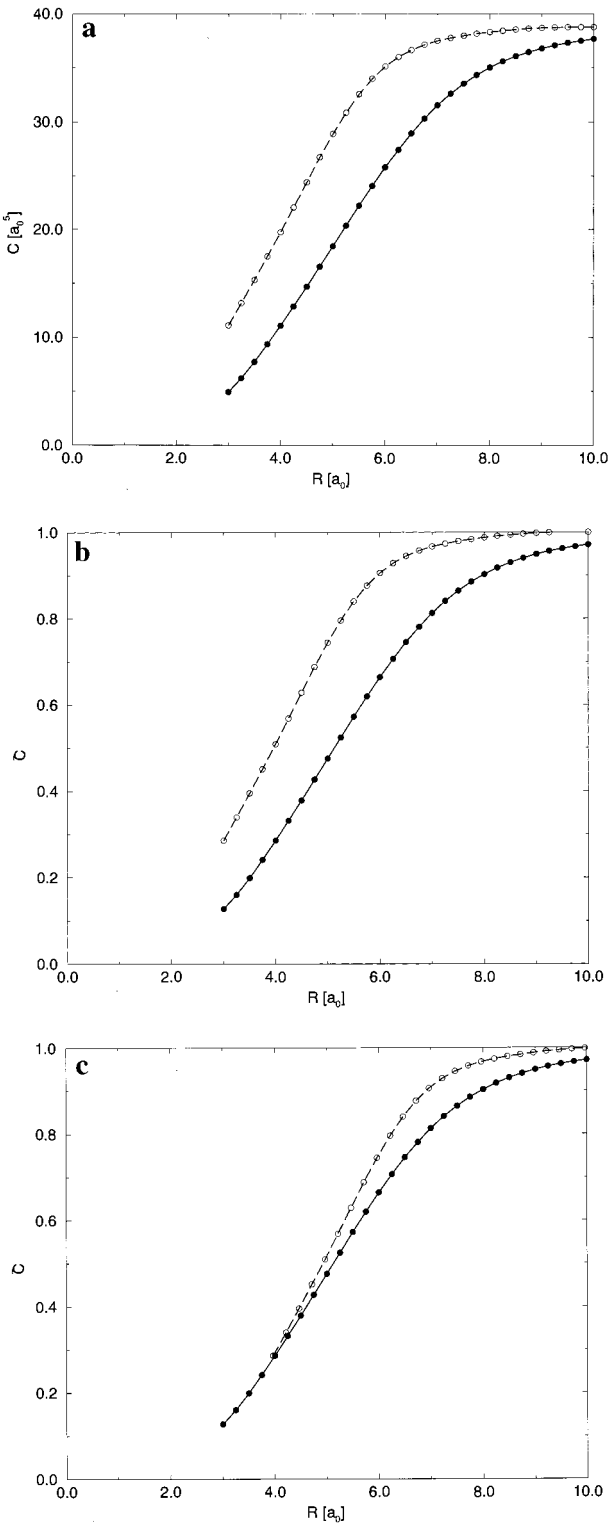

Figure 5. Quadrupole polarizability, $C(R)$, for F^- in LiF. (a) CRYS-(SCF) (○) and CLUS(SCF) (●), (b) scaling by the free ion value of C, (c) shifting by δ_{Li^+}.

For fluorides, chlorides, and bromides, the values are found to be independent of the anion and are $\sim 0.9a_0$, $1.2a_0$, and $1.7a_0$ for Li^+, Na^+, and K^+ cations in their salts, respectively. These values are somewhat smaller than the usually quoted crystal radii for these cations, but the trend is clearly correlated with ion size.

A further simplification of the data can be achieved if SCF and MP2 curves are mapped onto one another by a second translation $R \rightarrow R + \delta_2 R$ applied to the SCF data (Figure 3c).

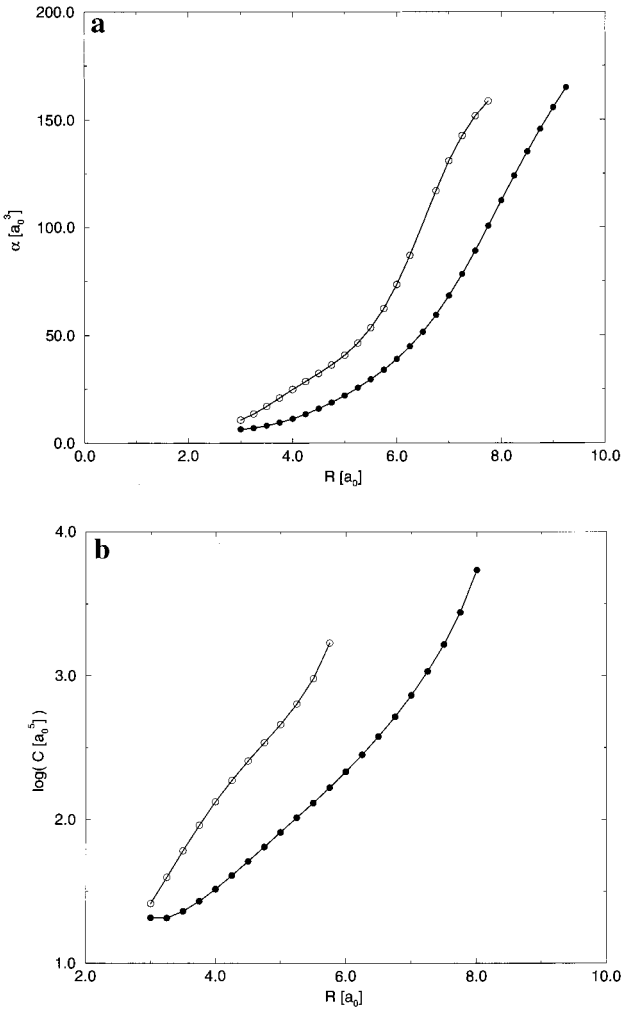

Figure 6. Dipole (a) and quadrupole (b) polarizabilities as a function of R for O^{2-} in MgO. Key: as for Figure 2; note the use of a logarithmic scale in panel b.

The practical attraction of this approach is clearly that, if the mapping is close, a sparse set of MP2 points could be used to "improve" an SCF curve. The shifts $\delta_2 R$ are found to be relatively insensitive to cation ($0.5a_0$ for Li^+, compared with $0.6a_0$ for Na^+), so that we can envisage unique polarizability functions for a given anion encompassing changes of counterion, level of correlation treatment, and sophistication of the crystal model. These "universal" curves for F^-, Cl^-, and Br^- are shown in Figure 4.

Similar qualitative considerations apply to the quadrupole polarizability C. As Figure 5 shows, the dependences of α and C on R have the same general sigmoid character, but C is more strongly affected by in-crystal compression for a given box size. This observation is in agreement with one-electron models.[10,11] It is interesting to note that the relatively simple CRYS → CLUS scaling procedure adopted successfully for the dipole polarizability curves is less successful for $C(R)$. This may, again, be characteristic of the greater dependence of C on the local environment. Future work will focus more on C.

Oxides. Table 1 gives the dipole polarizability at the equilibrium lattice parameter. The calculated dipole and quadrupole polarizabilities at the SCF level are shown in Figure 6.

The O^{2-} ion is unbound when not stabilized by the Madelung potential of a crystal lattice. Calculation of its polarizability at large lattice parameter, especially in the point charge only CRYS model, is, therefore, difficult and leads to numerical problems. Figure 6 shows the two SCF dipole polarizability curves for O^{2-} in MgO over the range where results were well converged. The same general trends noted earlier for all the halides still apply, but both curves are clearly diverging to a large, free ion value. The more tightly confined CLUS ion presents a more realistic picture here. It is worth stressing that the difficulties in calculation are significant only at unphysically high anion−cation separation and are not expected to degrade the results in the region of near-equilibrium geometries.

Scaling is problematic here, as the free ion polarizability (and, by implication, the value for any large R) is undefined for the correlated anion and restricted to a finite value for the uncorrelated anion only by the symmetry and limited basis set. However, one can still imagine translation by the cation radius (CRYS → CLUS) in the same manner as for the alkali halides. Using this procedure, a value of δ_{M^+} of 0.9 au for Mg^{2+} is found to bring the CRYS and CLUS curves into coincidence for $0 \leq R \leq 2R_e$. We do not have sufficient data to confirm, by checking its invariance from one material to another, that this parameter behaves as a cation property. However, the value is very similar to that obtained for Li^+, in agreement with chemical intuition for the radius of the Mg^{2+} ion.

As Figure 6b shows, the O^{2-} quadrupole polarizability is more strongly divergent than the dipole polarizability and is more sensitive to box size.

4. Comparison with Experiment

An experimental quantity related to $\alpha(R)$ is the dimensionless density derivative of the refractive index, $\rho(dn/d\rho)$.[25,26] The quantity available directly from our calculations is $d\alpha/dR$. The Lorentz−Lorenz relationship for a system of MX stoichiometry and cubic symmetry can be written

$$V_m\left(\frac{n^2-1}{n^2+2}\right) = \frac{4\pi}{3}\alpha_m = (\alpha_+ + \alpha_-) \qquad (4.1)$$

where V_m and α_m are the volume and polarizability per formula unit, respectively. Neglecting any pressure dependence of the cation polarizability, we find

$$\frac{d\alpha}{dR} = \frac{9R^2}{2\pi(n^2+2)}\left[(n^2-1) - \left(\frac{6n}{n^2+2}\right)\left(\rho\frac{dn}{d\rho}\right)\right] \qquad (4.2)$$

where $d\alpha/dR \equiv d\alpha_m/dR$ and, by the frozen cation assumption, $d\alpha_m/dR = d\alpha_-/dR$.

The experimental derivatives are also often expressed in terms of another dimensionless property, $-V_m d\epsilon_\infty/dV_m$ (see, for example, ref 29 and references therein), which is related to $\rho(dn/d\rho)$ by

$$2n\rho\frac{dn}{d\rho} = -V_m\frac{d\epsilon_\infty}{dV_m} \qquad (4.3)$$

Additionally, measurements are reported in terms of the Müller parameter, Λ_0, defined as $\Lambda_0 = (d \ln \alpha_m / d \ln V_m)$, which may be rewritten for our MX systems as $\Lambda_0 = (R/3\alpha_m)(d\alpha_m/dR)$. Hence, from eqs 4.1 and 4.2, the relationship between the experimental parameters is

$$\Lambda_0 = 1 - \left(\frac{6n}{(n^2+2)(n^2-1)}\right)\left(\rho\frac{dn}{d\rho}\right) \qquad (4.4)$$

Table 2 lists the data used to derive the experimental values of $d\alpha/dR$ for the systems under study. These are then compared

TABLE 3: Dipole Polarizability Derivatives, $(d\alpha/dR)/a_0^2$ [a]

	CRYS		CLUS		
system	SCF	MP2	SCF	MP2	expt
LiF	1.91 (0.179)	3.39 (0.201)	2.29 (0.214)	3.22 (0.191)	3.21−3.53
LiCl	4.92 (0.156)	6.59 (0.176)	5.50 (0.175)	6.46 (0.172)	9.85
LiBr	4.34 (0.113)	5.15 (0.124)	7.25 (0.189)	8.05 (0.193)	13.31
NaF	1.64 (0.154)	3.34 (0.198)	2.12 (0.200)−2.18 (0.205)	3.14 (0.187)−3.21 (0.191)	2.58−3.59
NaCl	3.62 (0.115)	5.09 (0.136)	5.11 (0.163)−5.32 (0.169)	6.05 (0.163)	6.73−7.62
NaBr	3.08 (0.080)	3.76 (0.090)	6.16 (0.161)−6.21 (0.162)	6.89 (0.165)−6.94 (0.166)	9.62−9.64
KF	1.19 (0.111)	2.78 (0.165)	2.30 (0.217)		4.32
KCl	2.28 (0.073)	3.41 (0.091)			6.34−8.45
KBr	2.05 (0.053)	2.61 (0.062)			7.93−8.68
MgO	15.30	24.89	7.77		11.435−11.900

[a] The numbers in parentheses are the (scaled) derivatives, $\alpha_\infty^{-1}(d\alpha/dR)/\alpha_0^{-1}$, where α_∞ is the polarizability of the free anion calculated at the appropriate level of theory and of simulation of the environment. The CLUS(MP2) calculations on NaX systems indicate the spread obtainable by using different estimates of BSSE where possible (see text).

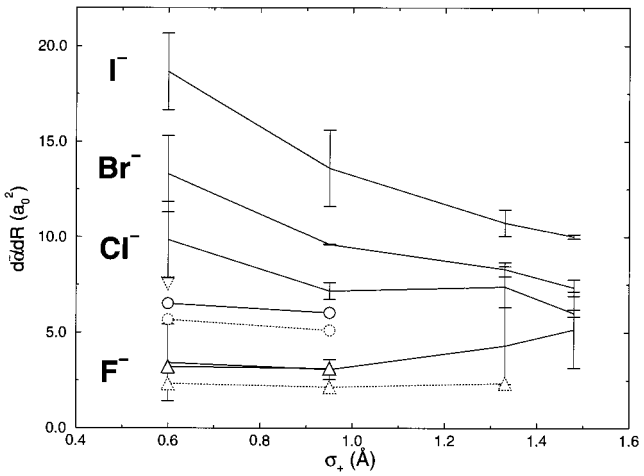

Figure 7. Ab initio SCF and MP2 dipole polarizability derivatives (lines with symbols) compared to the experimental values (solid lines, see Table 2). The error bars on the experimental data represent the range of values in Table 2. Key: △, F^- (solid, MP2; dotted, SCF); ○, Cl^- (solid, MP2; dotted, SCF); ▽, Br^- (SCF only shown).

in Table 3 with the calculated derivatives obtained at the various levels of theory. It can be seen that the MP2 derivatives are generally in much better agreement with experiment than are the SCF derivatives for the same systems. In passing, we note that the MP2 derivatives themselves are less sensitive to the modeling of anion−cation interactions (CRYS or CLUS); this is a natural consequence of the quenching of the anion correlation in the crystal. In general, the MP2 values for the derivatives appear to be smaller than those obtained from experiment by around 10%. This may reflect the growth in importance of correlation as the anion is given more freedom. A perturbative treatment such as MP2 will become progressively less accurate at large R, and although it is adequate for calculations of α_e, this inadequacy may influence $(d\alpha/dR)_e$.

Experimental data exist for a wider range of systems than we have been able to cover by ab initio calculation. Figure 7 places the calculated values into the more general context of the experimental data. The MP2 theoretical values are seen to be compatible with the experimental trends. Although the apparent agreement with the specific experimental values for LiCl and LiBr (Table 3) is relatively poor, the data for these systems (Table 2 from ref 28) are obtained via a slightly different procedure and appear systematically high.

In addition, the agreement between the experimental $(d\alpha/dR)$ for the O^{2-} ion in MgO and that calculated from CLUS(MP2) is also excellent, with the ab initio value slightly lower than that obtained from experiment, which is again consistent with the halide analysis above.

5. Constructing a Model

Several attempts have been made in the literature to construct models aimed at reproducing the volume dependence of the dipole polarizability. Two examples are the model of Wilson and Curtiss,[32] which uses, for the anion, a function of the form

$$\frac{\alpha_-}{\alpha_\infty} = \exp(-a/R^2) \tag{5.1}$$

and the Coker model,[33] which uses

$$\frac{\alpha_-}{\alpha_\infty} = (1 + aR^{-s})^{-1} \tag{5.2}$$

where a is a fitting parameter and s is an exponent fixed at 3 or 4. A fundamental problem with both functions is that they are unable to treat ions such as O^{2-}, which as free ions are unstable with respect to electron loss (i.e., $\alpha_\infty = \infty$). Furthermore, we are interested in constructing a model for the fluctuations in the polarizability in terms of a general set of ion coordinates, and, as a result, a more general expression is required.

Another possible function (the light-scattering (LS) model), as used previously by Madden and co-workers,[14] is based on the Drude model for the polarizability, in which the response of the charge density to an applied field is modeled by that of a harmonically bound charge q with force constant k. The polarizability is then given by $\alpha = q/k$. In the LS model, the confining effect of the ionic environment on the polarizability (Figure 1) is regarded as acting through the force constant, which, for a general ionic configuration, contains a part that depends on the separation between the ion of interest, i, and its neighbors.

$$k = k_0 + \sum_{j \neq i} a_{ij}\, e^{-c_{ij} r_{ij}} \tag{5.3}$$

where r_{ij} is the separation between ions i and j, a_{ij} and c_{ij} are parameters fitted to reproduce the dependence of the ab initio polarizability on the ionic environment, and $k_0 = 1/\alpha_\infty$. In a more general context, where the polarizability tensor may contain an anisotropic contribution, k would be replaced by a full second rank tensor. The LS model can, in principle, fit both sigmoidal (finite k_0) and divergent ($k_0 = 0$) polarizability curves, making it suitable for both bound and unbound anions. In keeping with the original LS model, we assume that only the nearest anion−anion and cation−anion interactions are

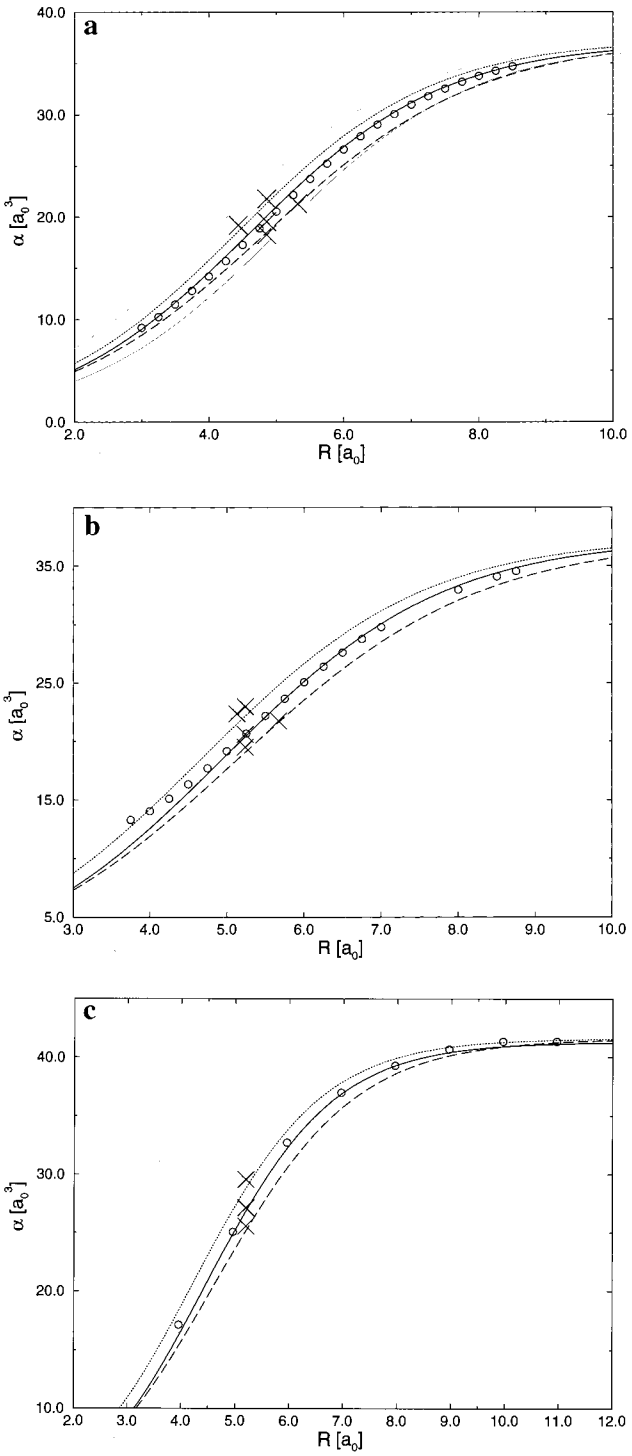

Figure 8. LS model fits to the ab initio MP2 data for (a) Cl^- in LiCl, (b) Cl^- in NaCl, and (c) Br^- in LiBr. Key: ○, current MP2 B1 ab initio; ×, Pyper and Popelier MP2 B1, B2, and B3 ab initio;[8] solid line, LS model fit to the B1 data; light dotted line, B3 LS model curve using anion−cation terms only; light gray dashes, B2 LS model fit using anion−cation terms only; corresponding black lines, fits using the full anion−cation and anion−anion terms.

significant in determining the polarizability of a central anion. This assumption can be tested by reference to the coordination number-dependent properties.

In another approach to the modeling of $\alpha(R)$, Batana and coworkers[37] have considered the experimental anion dipole polarizabilities in alkali halide crystals in terms of pressure-induced changes in the anion and cation radii. A detailed comparison of this work with the currect model will appear elsewhere.[38]

TABLE 4: LS Model Parameters Fitted to the CLUS(MP2) Data Using the Anion−Cation and Anion−Anion Interactions[a]

system	a_{+-} (a_0^{-3})	c_{+-} (a_0^{-1})	a_{--} (a_0^{-3})	c_{--} (a_0^{-1})	k_0 (a_0^{-3})
LiF	0.190	0.810	0.095	0.573	0.0595
NaF	0.235	0.810	0.095	0.573	0.0595
LiCl	0.060	0.700	0.030	0.495	0.0268
NaCl	0.074	0.700	0.030	0.495	0.0268
MgO	0.120	0.680	0.060	0.550	0.0
KF	0.363	0.810	0.095	0.573	0.0595
LiBr	0.090	0.850	0.045	0.601	0.0242

[a] The values for both KF and LiBr are fitted to effective CLUS(MP2) curves generated from the CRYS(MP2) as described in the text.

Representation with the LS Model. Figure 8 shows the fit of the LS model to the ab initio CLUS(MP2) data for LiCl. Equation 5.3 becomes, for the shortest-ranged cation−anion and anion−anion interactions of the B1 structure,

$$k(R) = k_0 + 6a_{+-}\,e^{-c_{+-}R} + 12a_{--}\,e^{-\sqrt{2}c_{--}R} \qquad (5.4)$$

where both the anion−cation (a_{+-},c_{+-}) and anion−anion (a_{--},c_{--}) parameters are fitted. One can, of course, fit the ab initio B1 data using only the anion−cation terms in this equation while retaining the same quality of fit, since for a fixed structure the anion−cation and anion−anion nearest neighbor distances are related by a constant factor. However, additional ab initio points are available from the work of Pyper and Popelier,[8] who have calculated anion dipole polarizabilities for three cubic crystal structures of LiCl and other systems. When these data are incorporated, it is found that a single-exponential anion−cation model cannot reproduce the B3 (four-coordinate) and B2 (eight-coordinate) data as closely as that for the B1 structure. The model at this level is not flexible enough to be transfered to different coordination environments. The more flexible function, including both the anion−cation and anion−anion interactions, is able to reproduce the four-, six-, and eight-coordinate values. The additional flexibility arises because of the different weightings of the anion−cation and anion−anion functions in the different crystal structures (in terms of both relative separations and coordination numbers).

Table 4 lists the full parameter sets derived from eq 5.3 by fitting to the MP2 CLUS data in the rocksalt structure. The fact that the polarizability data for a given anion have been shown to scale for different cations encourages us to think that the parameters for different cations would be related, and this is borne out by the fit. In fact, the c parameters can be considered to be cation-independent and the preexponential factors simply related for a given anion. We found that the Na^+ salt preexponential factors are simply obtained from those for the Li^+ salts by scaling in terms of the effective cation radii obtained from δ_{M^+} shifts described earlier, i.e., $a_{Na^+X^-} = a_{Li^+X^-} \exp[c_{Li^+X^-}(\delta_{Na^+} - \delta_{Li^+})]$. For example, Figure 8b compares the ab initio NaCl data with the LS model scaled in this way. The models clearly transform well between systems, allowing the generation of new data sets without lengthy calculation.

Predictions from the LS Model. To test the validity of these scaling procedures, we consider the LiBr system, for which only CRYS data are available at the MP2 level. An estimate of the CLUS(MP2) curve for $\alpha(R)$ is obtained in Figure 8c by shifting the CRYS(MP2) values in terms of the cation radius. Also shown in the same figure are the three ab initio points from Pyper and Popelier,[8] corresponding to the dipole polarizability of the bromide anion in the B1, B2, and B3 structures calculated at the equilibrium B1 anion−cation separation. It is clear that

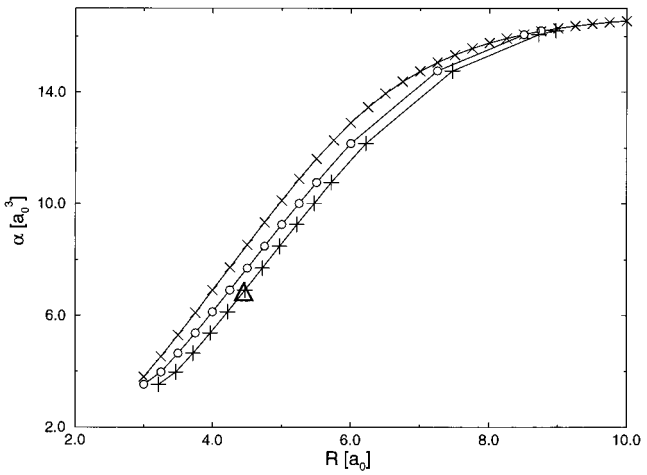

Figure 9. LS model fit for F^- in CaF_2 constructed from the current LiF and NaF ab initio as described in the text. Key: ×, LiF MP2; ○, NaF MP2; +, scaled onto single CaF_2. The experimental equilibrium α is shown as (△).

the scaled CLUS curve passes through the single ab initio B1 point, and also that the full LS model is again able to account for the coordination number dependence.

To explore the transferability of the "universal" $\alpha(R)$ curve, we take the example of the F^- ion in CaF_2, for which an experimental Müller parameter is available.[34] In Figure 9 the LiF curve for $\alpha(R)$ from Figure 2 is shifted to reproduce the experimental anion polarizability for F^- in CaF_2 at the experimental equilibrium lattice parameter. The calculated $d\alpha/dR$ is around $3.1a_0^2$, compared with $2.6a_0^2$ from the experiment,[34] demonstrating the usefulness of the procedure.

6. Summary

We have presented results for the variation of the mean polarizability, α, of an in-crystal anion with lattice parameter R obtained for two levels of representation of the crystalline environment (CRYS and CLUS) and at two levels of ab initio theory (SCF and MP2). The CRYS environment is simply that of a lattice of point charges surrounding the anion of interest, whereas the CLUS further includes the effect of the full electron density of the first shell of nearest-neighbor cations. At the highest level of theory, CLUS(MP2), the results for $d\alpha/dR$ are in excellent agreement with experiment.

It was shown that a series of physically motivated scaling procedures could be performed on the values of $\alpha(R)$ obtained at different levels of calculation *and* for different cations with the same anion, so that all the results for a given anion could be reduced to a single universal curve. This scaling validates a representation of the influence of the environment on the polarizability of the anion as a consequence of a simple confining (pseudo) potential, whose width is determined simply by the lattice parameter and by a radius, δ_{M^+}, characteristic of the cation electron density.

Based upon this finding, a functional form was proposed to express the polarizability in terms of the nearest-neighbor cation−anion and anion−anion separations. The functional form was then used to predict the polarizability in other crystal structures, and good agreement between these predictions and ab initio determined polarizabilities was found. For a given anion, the parameters in the function for different cations were simply related through the change in cation radius, δ_{M^+}. The function is, therefore, able to predict the polarizability in different substances and crystal structures.

Acknowledgment. The authors thank Dr. N. C. Pyper for sending copies of his work prior to publication. P.W.F. thanks Professor R. W. Munn for helpful discussions. The work was supported by EPSRC Grant GR/L/05068. M.W. thanks the Royal Society for a Research Fellowship.

References and Notes

(1) Mahan, G. D. *Solid State Ionics* **1980**, *1*, 29.
(2) Mahan, G. D.; Subbaswamy, K. R. *Local Density Theory of Polarizability*; Plenum: London, 1990.
(3) Fowler, P. W.; Madden, P. A. *Phys. Rev. B* **1985**, *31*, 5443.
(4) Fowler, P. W.; Madden, P. A. *Mol. Phys.* **1983**, *49*, 913.
(5) Fowler, P. W.; Madden, P. A. *Phys. Rev. B* **1984**, *29*, 1035.
(6) Fowler, P. W.; Madden, P. A. *Phys. Rev. B* **1984**, *30*, 6131.
(7) Fowler, P. W.; Tole, P. *Mol. Phys.* **1990**, *86*, 1019.
(8) Pyper, N. C.; Popelier, P. *J. Phys.: Condens. Matter*. **1997**, *9*, 471.
(9) Fowler, P. W.; Pyper, N. C. *Proc. R. Soc. A* **1985**, *398*, 377.
(10) Fowler, P. W. *Mol. Phys.* **1984**, *53*, 865.
(11) Fowler, P. W. *Mol. Phys.* **1985**, *54*, 129.
(12) Wilson, M.; Madden, P. A. *J. Chem. Soc., Faraday Trans.* **1997**, *106*, 339.
(13) Wilson, M. *J. Phys. Chem. B* **1997**, *101*, 4917.
(14) Madden, P. A.; O'Sullivan, K.; Board, J. A.; Fowler, P. W. *J. Chem. Phys.* **1991**, *94*, 918−927.
(15) Wilson, M.; Exner, M.; Huang, Y.-M.; Finnis, M. W. *Phys. Rev. B* **1996**, *54*, 15683.
(16) Wilson, M.; Schönberger, U.; Finnis, M. W. *Phys. Rev. B* **1996**, *54*, 9147.
(17) Rowley, A. J.; Jemmer, P.; Wilson, M.; Madden, P. A. *J. Chem. Phys.*, to be published.
(18) Wilson, M.; Cabral, B. J. C.; Madden, P. A. *J. Phys. Chem.* **1996**, *100*, 1227.
(19) CADPAC: The Cambridge Analytic Derivatives Package Issue 6, Cambridge, 1995 (a suite of quantum chemistry programs developed by R. D. Amos with contributions from I. L. Alberts, J. S. Andrews, S. N. Colwell, N. C. Handy, D. Jayatilaka, P. J. Knowles, R. Kobayashi, K. E. Laidig, G. Laming, A. M. Lee, P. E. Maslen, C. W. Murray, J. E. Rice, E. D. Simandiras, A. J. Stone, M.-D. Su, and D. J. Tozer.)
(20) Lazzeretti, P.; Malagoli, M.; Zanasi, P. CNR Technical Report on Project "Sistemi Informatici e Calcolo Parallelo", CNR, Rome, 1991; 1/67.
(21) Müller, U. *Inorganic Structural Chemistry*; Wiley: Chichester, 1993.
(22) Fowler, P. W.; Madden, P. A. *J. Phys. Chem.* **1985**, *89*, 2581.
(23) Boys, S. F.; Bernardi, F. *Mol. Phys.* **1970**, *19*, 553.
(24) Buckingham, A. D. *Adv. Chem. Phys.* **1967**, *12*, 107.
(25) Johannsen, P. G. *Phys. Rev. B* **1997**, *55*, 6856.
(26) Johannsen, P. G.; Reiss, G.; Bohle, U.; Magiera, J.; Müller, R.; Spiekermann, H.; Holzapfel, W. B. *Phys. Rev. B* **1997**, *55*, 6865.
(27) Bendow, B.; Gianino, P. D.; Tsay, Y. F.; Mitra, S. S. *Appl. Opt.* **1974**, *13*, 2382.
(28) Fontanella, J.; Andeen, C.; Schuele, D. *Phys. Rev. B* **1972**, *6*, 582.
(29) Shanker, J.; Agrawal, G. G.; Singh, R. P. *Philos. Mag. B* **1979**, *39*, 405.
(30) Singh, A. V.; Sharma, J. C.; Shanker, J. *Physica* **1978**, *94B*, 331.
(31) Van Vechten, J. A. *Phys. Rev.* **1969**, *182*, 891.
(32) Wilson, J. N.; Curtiss, R. M. *J. Phys. Chem.* **1970**, *74*, 187.
(33) Coker, H. *J. Phys. Chem.* **1976**, *80*, 2078.
(34) Balzaretti, N. M.; Da Jornada, J. A. H. *J. Phys. Chem. Solids* **1996**, *57*, 179.
(35) Balzaretti, N. M.; Da Jornada, J. A. H. *High-Pressure Res.* **1990**, *2*, 183.
(36) Pyper, N. C. *J. Phys.: Condens. Matter*, **1995**, *7*, 9127. Wilson, N. T.; Wilson, M.; Madden, P. A.; Pyper, N. C. *J. Chem. Phys.* **1996**, *105*, 11209.
(37) Batana, A.; Bruno, J.; Munn, R. W. *Mol. Phys.* **1997**, *92*, 1029.
(38) Batana, A.; Fowler, P. W. Jemmer, P.; Madden, P. A.; Munn, R. W.; Wilson, M., manuscript in preparation.